ARTICLES

Nanostructured, Gd-Doped Ceria Promoted by Pt or Pd: Investigation of the Electronic and Surface Structures and Relations to Chemical Properties

Holger Borchert,*,† Yulia Borchert,†,‡ Vasiliy V. Kaichev,† Igor P. Prosvirin,† Galina M. Alikina,† Anton I. Lukashevich,† Vladimir I. Zaikovskii,† Ella M. Moroz,† Eugenii A. Paukshtis,† Valerii I. Bukhtiyarov,† and Vladislav A. Sadykov†,‡

Boreskov Institute of Catalysis, SB RAS, Novosibirsk, Russia, and Novosibirsk State University, Novosibirsk, Russia

Received: March 24, 2005; In Final Form: August 29, 2005

Nanostructured ceria doped with other rare earth elements is a good oxygen ion conductor, which gives rise to various catalytic applications such as the construction of membranes for syngas production by partial oxidation of methane. This article focuses on the Gd-doped cerium dioxides, which can be modified with Pt or Pd to enhance the reactivity of the lattice oxygen in interaction with methane. The aim of the work is the elucidation of correlations between the structural, electronic, and chemical properties of these nanomaterials. Detailed studies were performed for a series of samples with and without surface modification by noble metals using a complex combination of physicochemical methods: XRD, TEM, CH_4 TPR, XPS, SIMS, and FTIR spectroscopy of adsorbed CO. XPS and TPR data revealed that surface modification with noble metals enhances the reducibility of the doped ceria support, where the effect is more pronounced for Pd than for Pt. The formation of highly cationic Pd species due to strong metal support interactions provides a possible explanation for this behavior. Furthermore, the results obtained in the present work for the Gd-doped ceria system are compared to those obtained previously for the Pr-doped ceria system.

1. Introduction

Materials based on ceria are widely used for a variety of catalytic applications such as three-way catalysts,[1] selective oxidation or dehydrogenation of organic compounds,[2,3] solid oxide fuel cells,[4] and membranes for efficient synthesis gas generation by partial oxidation of methane.[5,6] Many of these applications are due to the high oxygen ion conductivity and oxygen storage capacity, which can easily be achieved in ceria by doping with other rare earth elements such as Gd, Pr, Sm, etc., which creates oxygen vacancies and enables migration of oxygen ions through the lattice.[7−9]

Particular attention is currently attracted by *nanostructured* ceria-based materials.[3,10−14] Reduction of the size to the nanometer scale can lead to chemical and physical properties that differ from those of the corresponding bulk materials. This opens new possibilities to further modify and improve the materials with respect to possible catalytic applications. Recently, we reported on nanostructured ceria doped with Sm,[15] Bi,[15] Pr,[16,17] and Gd[18,19] prepared by the so-called "Pechini method".[20] The materials exhibit high oxygen ion conductivity with the lattice oxygen mobility depending on the kind and amount of dopant ions. Furthermore, the reactivity of the lattice oxygen in the interaction with methane can be modified by promotion of the doped ceria with Pt or Pd.[15−19] This is quite important for possible catalytic applications such as methane conversion into synthesis gas.

Detailed analysis is required to elucidate how the electronic and surface structures and the reactivity with respect to oxidation of methane are influenced by the kind and amount of dopant ions, as well as by surface modification with noble metals. Such an investigation of the electronic and chemical properties has successfully been performed and recently been reported for the Pr-doped system.[21] Based on surface science studies, a model that explains the different chemical behaviors induced by surface modification with platinum was suggested.[21]

With similar intentions, we now address the Gd-doped system. Nanostructured Gd-doped cerium dioxides with and without promotion by platinum and palladium were investigated by X-ray photoelectron spectroscopy (XPS) and Fourier transform infrared (FTIR) spectroscopy of adsorbed carbon monoxide. The catalytically relevant redox properties of the doped cerium dioxides were studied by temperature-programmed-reduction (TPR) techniques. Bulk structures of the samples were examined by powder X-ray diffraction (XRD) and transmission electron microscopy (TEM). Furthermore, secondary-ion mass spectrometry (SIMS) was used to study the segregation of the dopant ions on the surface.

2. Experimental Section

Samples of highly dispersed gadolinium-doped ceria were prepared by a polymerized complex precursor route known as

* Corresponding author. Present address: Department of Pure and Applied Chemistry, Physical Chemistry 1, Carl-von-Ossietzky-Str. 9-11, 26129 Oldenburg, Germany. E-mail: Holger_Borchert@gmx.net.

† Boreskov Institute of Catalysis.

‡ Novosibirsk State University.

10.1021/jp051525m CCC: $30.25
Published on Web 10/12/2005

the Pechini method[20] and calcined at 500 °C. Details of the sample preparation are presented elsewhere.[22] Briefly, cerium nitrate and gadolinium nitrate were dissolved in a mixture of citric acid and ethylene glycol ("pure for chemical analysis" grade, Russia). Addition of ethylenediamine and careful heating leads to the formation of a polymerized matrix surrounding the precursors. Calcination removes the organic matrix and yields nanostructured doped ceria.[22] Various samples are compared in the present work: pure cerium oxide, pure gadolinium oxide, and Gd-doped ceria samples with 10−50% Gd content (amount of Gd used in the synthesis). The latter were studied in three modifications: without surface modification, promoted with 1.4 wt % Pt, and promoted with 1.4 wt % Pd supported by incipient wetness impregnation.[22]

The samples were studied by powder X-ray diffraction, transmission electron microscopy (TEM), X-ray photoelectron spectroscopy (XPS), secondary-ion mass spectrometry, Fourier transform infrared spectroscopy of adsorbed CO probe molecules, and temperature-programmed reduction in a CH_4/He flow.

The XRD experiments were performed using a URD-6 diffractometer with monochromated Cu Kα irradiation. A JEOL JEM-2010 transmission electron microscope operated at 200 kV was used for TEM studies. Samples for the TEM measurements were prepared by ultrasonicating a small quantity of the powder for a few minutes in ethanol. The resultant slurry was then deposited on a copper grid.

The XPS experiments were performed with a VG ESCALAB HP spectrometer equipped with a hemispherical electron analyzer and an aluminum anode ($h\nu = 1486.6$ eV) operated at 200 W. Before the measurements, the spectrometer was calibrated using the Au $4f_{7/2}$ binding energy (BE) of 84.00 eV and the Cu $2p_{3/2}$ BE of 932.67 eV measured for clean gold and copper foils as references. All investigations were carried out at room temperature and at pressures typically below 10^{-7} mbar. The resolution was about 1.2 eV. Since no carbon peaks were observed, the constant energy shift caused by the charging effect (up to ~15 eV) was corrected by referencing all the binding energies to the well-pronounced Ce $3d_{3/2}$ u‴ feature at 916.7 eV.[21] The experimental XPS spectra discussed in this article were deconvolved into individual components using Voigt line shapes. Quantitative analysis was performed from the integral intensities of the XPS peaks corrected by the atomic sensitivity factors of the corresponding elements.[23]

Powder samples were pressed into spoonlike copper sample holders or rubbed into a Ni mesh fixed on a copper sample holder. The samples were investigated by XPS after two different treatments, with oxygen and methane, which were carried out in situ, i.e., in the preparation chamber of the photoelectron spectrometer. During the oxidation treatment, the samples were exposed to 5000 Pa of O_2 at 400 °C for 1 h. Afterward, the samples were cooled to room temperature before the gas was pumped off and the sample was transferred into the analyzer chamber, where spectra were recorded in vacuo. (About ~30 min passed after the removal of the gas before spectra could be recorded.) For the in situ treatment with methane, the samples were heated to the highest accessible temperature of about 540 °C and exposed to 5000 Pa of CH_4 for 1 h. After addition of methane, the temperature dropped to ~490 °C after several minutes. Samples were finally cooled to room temperature before the gas was pumped off. It should be noted that no indications of carbon deposition after the methane treatment were found by XPS.

For SIMS, powder samples were rubbed into a high-purity indium substrate. An argon ion beam with energy of 3 keV and current density of 5 μA/cm^2 was used for the sputtering of the samples. The detection of the secondary ions was performed with a MC-7201 monopole mass spectrometer. The signals at m/z values of 140 and 160 units were assigned to secondary-ion currents of cerium and gadolinium ions, respectively. The thickness of the layer etched out by argon bombardment was calculated from the sputtering time as described elsewhere.[24]

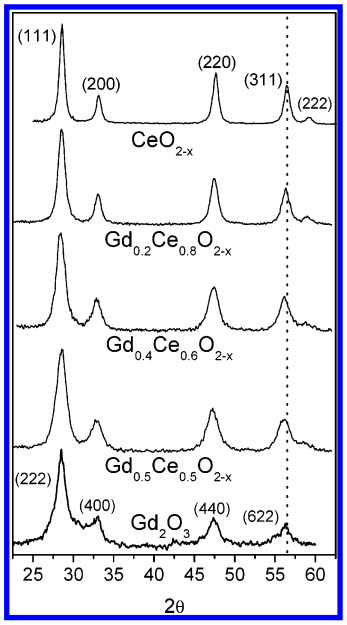

Figure 1. XRD patterns of nanostructured cerium oxide, gadolinium oxide, and doped ceria with different Gd contents.

The FTIR spectra of adsorbed CO were obtained at 77 K using a Shimadzu FTIR-8300 spectrometer with a resolution of 4 cm^{-1}. Powder samples were pressed into self-supported wafers, which were pretreated in a vacuum during 90 min at 500 °C in situ in a specially designed IR cell. The CO adsorption was performed by introduction of small doses of CO.

The TPR experiments were carried out in a specially designed flow reactor. In a first step, 0.3 g of a given sample was pretreated for 40 min at 450 °C in a gas mixture of 1% oxygen in helium at a flux rate of 10 L/h. The sample was then cooled to room temperature in the oxygen/helium mixture. After this pretreatment, temperature-programmed reduction was performed with a gas mixture of 1% methane in helium at a flux rate of 10 L/h. The temperature was linearly increased at a rate of 5 °C/min. Samples were finally kept for 70 min at the highest temperature of 880 °C. The gas mixture was analyzed with an IR absorbance gas analyzer. Results for the main reaction products CO and CO_2 are expressed in terms of consumed oxygen provided from the doped cerium oxide samples.

3. Results and Discussion

3.1. Structural Features. Figure 1 shows XRD patterns of cerium and gadolinium oxides and doped ceria samples with different Gd contents. The cerium oxide and all doped samples were found to be single-phased and to possess a fluorite-like structure. The lattice parameter was found to increase with the dopant content (see Table 1),[18] the variation being in quantitative agreement with observations in rare earth doped ceria made by McBride et al.[25] The increase in the lattice parameter is reflected in Figure 1 by a slight shift of the XRD reflections and demonstrates the incorporation of the relatively large Gd^{3+} ions into the ceria lattice.[18,25] The XRD pattern of the pure gadolinium oxide sample reveals the formation of Gd_2O_3 with a more

TABLE 1: Lattice Parameters and Domain Sizes As Determined by the Scherrer Equation for Undoped and Doped Nanostructured Oxide Materials

sample	domain size [nm]	lattice parameter *a* [Å]
CeO_{2-x}	17.0	5.411
$Gd_{0.1}Ce_{0.9}O_{2-x}$	11.5	5.418
$Gd_{0.2}Ce_{0.8}O_{2-x}$	9.0	5.422
$Gd_{0.3}Ce_{0.7}O_{2-x}$	8.5	5.421
$Gd_{0.4}Ce_{0.6}O_{2-x}$	7.0	5.431
$Gd_{0.5}Ce_{0.5}O_{2-x}$	5.5	5.435
Gd_2O_3	6.0	10.856

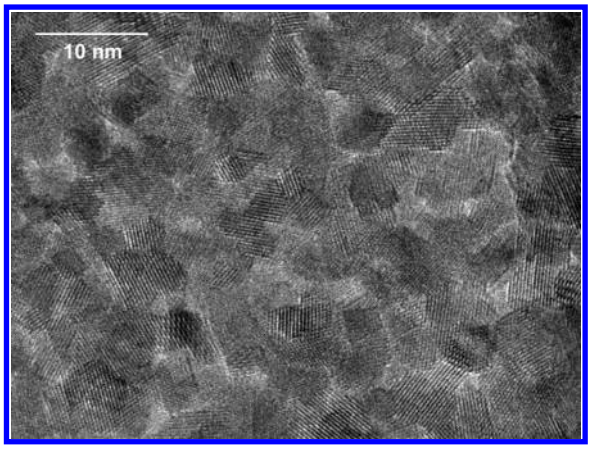

Figure 2. High-resolution transmission electron micrograph of the doped cerium dioxide sample with 20% Gd content. Clearly resolved lattice fringes indicate a high degree of crystallinity within the domains of the nanostructured oxide.

complex cubic structure, which can be derived from the fluorite structure by removal of a quarter of the anions. The lattice parameter is doubled with respect to the fluorite structure due to an ordered arrangement of the anion vacancies. The (222) and (400) reflections (which correspond to (111) and (200), when the lattice parameter is not doubled) are not as clearly resolved as for the other samples; a strong background fills in the tail between the two reflections. This indicates the coexistence of an amorphous phase and the crystalline phase for the pure gadolinium oxide sample.

A high-resolution TEM image of doped cerium dioxide with 20% Gd content is shown in Figure 2. One can clearly see nanocrystalline domains sintered into platelets with a large number of probably disordered domain boundaries. Within the domains, the sample presents a high degree of crystallinity as revealed by the clearly visible lattice fringes.

Average sizes of the nanocrystalline domains (shown in Table 1) were estimated from the width of the (311) reflection according to the Scherrer equation as described in ref 21. For the doped samples, a systematic decline of the average domain size with increasing Gd content is found.[18] This suggests that Gd tends to segregate at the domain boundaries, which hinders further growth of the domains. A precise comparison of the domain size as obtained by XRD and TEM is difficult because of the rather broad size distribution. Nevertheless, both methods unambiguously show that the Pechini method provides a synthesis route for highly dispersed, nanostructured, Gd-doped cerium dioxides.

SIMS and XPS were used to examine the segregation of the dopant ions in the host lattice. At all Gd contents, SIMS revealed an enhanced Gd-to-Ce ion current ratio at the beginning of the sputtering, which provides a clear indication for segregation of gadolinium ions at the surface.[26] After the removal of about ~1 nm of substance, the ion current ratio reached a more or less constant level in all cases, which indicates a rather homogeneous distribution of the Gd ions in the volume of the nanocrystalline domains.[26]

Segregation of gadolinium ions at the surface was confirmed by XPS. The results of the quantitative analysis based on the total areas of the Gd 3d and Ce 3d peaks are presented in Table 2. The [Gd]/[Ce] atomic ratio is up to 2 times higher than the theoretical ratio for the case of homogeneous distribution of the dopant ions in the host lattice. The segregation effect seems to be slightly more pronounced in the samples promoted by Pt or Pd. In some cases, the atomic ratio of Gd to Ce as determined by XPS decreases after the treatment of the samples with methane. As will be shown in section 3.3.2, this occurs in those cases where the methane treatment leads to considerable reduction of Ce^{4+} to Ce^{3+} cations (see also Table 2).

It is interesting to compare these results with the case of Pr-doped ceria, where the effect of segregation of the dopant ions was *enhanced* after reduction of the samples with methane. It is possible that Pr cations tend to segregate to the surface when they are reduced from Pr^{4+} to Pr^{3+}.[21] Since no compounds are known with Gd in the +4 oxidation state, an analogous process does not proceed in the Gd-doped ceria. Instead, the decrease in the Gd-to-Ce ratio after the reductive treatment suggests that cerium tends to segregate to the surface when it is reduced from Ce^{4+} to Ce^{3+}.

Comparing the Gd- and Pr-doped ceria systems,[21] one can also notice that the segregation effect is more pronounced in the Gd-doped system. This is a reasonable result, because Pr can partly be incorporated in the form of Pr^{4+} cations which match much better to the ceria lattice than the relatively large Pr^{3+} and Gd^{3+} cations.

3.2. Chemical Behavior with Respect to Catalytic Conversion of Methane. Recently it was shown that nanostructured cerium dioxide doped with different rare earth elements and promoted with noble metals may serve as an efficient catalyst for synthesis gas generation via selective oxidation as well as steam or dry reforming of methane.[17,19] The syngas yield was found to depend on the lattice oxygen mobility, which in turn can be tuned in the nanostructured ceria system by the appropriate choice of the kind and amount of dopant ions.[16−19] To further investigate the catalytically relevant redox properties of the Gd-doped ceria, additional temperature-programmed-

TABLE 2: Atomic Ratios of Gd to Ce (Determined by XPS after Treatment with O_2 and CH_4 and Calculated for the Theoretical Case of Homogeneous Spatial Distribution of the Dopant Ions in the Host Lattice) and Atomic Fractions of Ce Ions in the +3 Oxidation State

	atomic ratio of Gd to Ce			$[Ce^{3+}]/[Ce^{3+}+Ce^{4+}]$ [%]	
sample	after O_2 treatment	after CH_4 treatment	homogeneous distribution	after O_2 treatment	after CH_4 treatment
CeO_{2-x}				8.0	
$Gd_{0.4}Ce_{0.6}O_{2-x}$	0.93	0.93	0.67	1.5	4.5
$Pt/Gd_{0.2}Ce_{0.8}O_{2-x}$	0.54	0.50	0.25	4.5	9.5
$Pt/Gd_{0.4}Ce_{0.6}O_{2-x}$	1.16	1.04	0.67	2.5	13.5
$Pd/Gd_{0.2}Ce_{0.8}O_{2-x}$	0.54	0.41	0.25	11.5	27.0
$Pd/Gd_{0.4}Ce_{0.6}O_{2-x}$	1.23	0.91	0.67	11.0	25.0

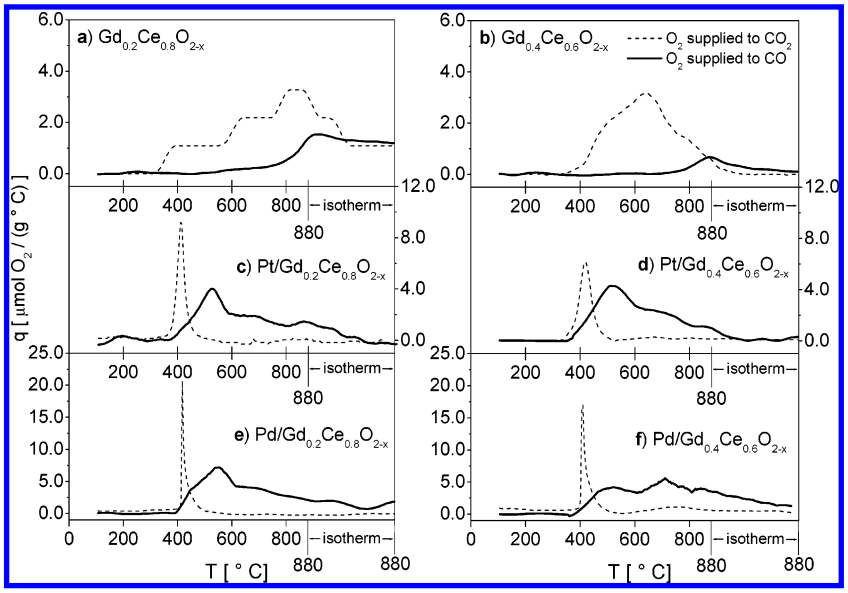

Figure 3. Results of temperature-programmed-reduction experiments with methane for Gd-doped ceria samples without surface modification (a, b), promoted by platinum (c, d), and promoted by palladium (e, f). On the ordinate is plotted the amount of oxygen supplied from the samples which after the reaction is present in form of CO_2 (dashed lines) and CO (solid lines). The data are normalized to 1 g of substance.

TABLE 3: Amounts of Oxygen Converted in the TPR Run to CO and CO_2 and Rates of Reduction at the Maximum of the First TPR Peak for Gd-Doped Ceria Samples

	oxygen converted in TPR run [mmol of O_2/g]		max reduction rate [10^{16} O atoms/m^2·s]	
sample	Q(CO)	Q(CO_2)	W_{max}(CO)	W_{max}(CO_2)
$Gd_{0.2}Ce_{0.8}O_{2-x}$	0.57	1.48	0.8	1.6
$Gd_{0.4}Ce_{0.6}O_{2-x}$	0.23	1.06	0.2	0.8
$Pt/Gd_{0.2}Ce_{0.8}O_{2-x}$	1.12	0.39	2.3	5.2
$Pt/Gd_{0.4}Ce_{0.6}O_{2-x}$	1.27	0.43	1.0	1.6
$Pd/Gd_{0.2}Ce_{0.8}O_{2-x}$	2.68	0.42	4.0	11.5
$Pd/Gd_{0.4}Ce_{0.6}O_{2-x}$	2.49	0.77	1.4	4.0

reduction experiments have been performed using 1% CH_4 in He as a reducing agent.

Figure 3 shows CH_4 TPR profiles for a series of various samples. The results are expressed in terms of oxygen supplied from the sample to the two main oxidation products: carbon monoxide (desired reaction, syngas generation by the partial oxidation of methane: $CH_4 + (1/2)O_2 \rightarrow CO + 2H_2$) and carbon dioxide (concurrent reaction, deep oxidation of methane: $CH_4 + 2O_2 \rightarrow CO_2 + 2H_2O$). For Gd-doped ceria (Figure 3a,b), the deep oxidation of methane to carbon dioxide begins at moderate temperatures around ~400 °C, while considerable production of synthesis gas starts only at high temperatures around ~750 °C. Promotion of the samples by 1.4 wt % Pt drastically affects these characteristics. The partial oxidation of methane dominates already at ~450 °C (Figure 3c,d). CO_2 formation is observed as a sharp reduction peak around 400 °C. A rather similar effect is achieved by surface modification with Pd (Figure 3e,f). As an important difference between the Pt- and Pd-promoted samples, one can notice, however, that the total amount of oxygen supplied to CO during the TPR run, Q(CO), is ~2 times higher in the case of surface modification with Pd (see Table 3). The reduction rates at the maxima of the first TPR peaks, W_{max}(CO) and W_{max}(CO_2), are also considerably enhanced for the Pd-promoted samples (see Table 3). Comparing samples with different Gd contents, note, furthermore, that the maximum reduction rates are higher at 20% Gd content where the lattice oxygen mobility is higher.[18]

Our recent investigations of the electronic and surface structures of the Pr-doped system revealed that partial oxidation and deep oxidation of methane involve the preferential reduction of cerium and praseodymium cations, respectively.[21] On the basis of this observation, it was possible to suggest a model for different reaction mechanisms in the presence or absence of noble metals on the surface. While deep oxidation to carbon dioxide was found to be likely when methane adsorbs on the defect-rich domain boundaries, partial oxidation to carbon monoxide seemed to be favored by activation of methane at Pt sites on the regular surface.[21]

In the following, we present investigations of the electronic and surface structures of Gd-doped ceria to achieve also for this system a better understanding of the influence of the dopant content and of the effects of surface modification with noble metals on the chemical behavior in contact with methane.

3.3. Electronic and Surface Structures. *3.3.1. Gadolinium Oxide.* In our XPS investigations we use pure cerium and gadolinium oxides prepared by the Pechini method as references. While undoped nanostructured cerium dioxide has been studied previously,[21] the electronic and surface properties of Gd_2O_3 are examined by XPS here. Figure 4a shows a photoelectron Gd 3d spectrum recorded after the in situ oxidative pretreatment of the sample. The spectrum was fitted using a combined polynomial and Shirley-type background function and four doublets of Voigt peaks labeled a/b, a′/b′, a″/b″, and a_S/b_S. A value of 0.5 eV was used for the Lorentzian width of all peaks. Since no other charge reference was available for the *pure* gadolinium oxide sample, the binding energy scale was calibrated in this case by assigning a literature value of 530.4 eV to the main O 1s peak (Figure 4b).[27,28] Spectra of the *doped* samples were referenced to the Ce $3d_{3/2}$ u‴ feature at 916.7 eV.

The Gd 3d spectrum of pure gadolinium oxide presents a main doublet a/b with the $3d_{5/2}$ peak centered at 1187.2 eV and

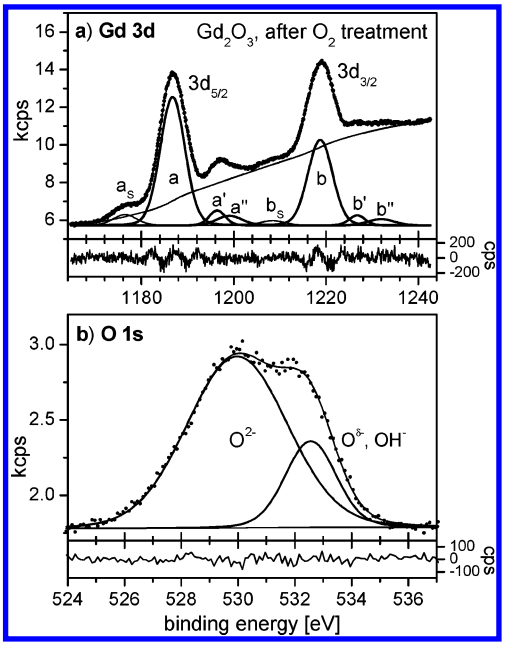

Figure 4. XPS Gd 3d (a) and O 1s spectra (b) of the Gd_2O_3 sample after pretreatment with oxygen. The energy scale has been calibrated by setting a literature value of 530.4 eV to the binding energy of the main O 1s peak.

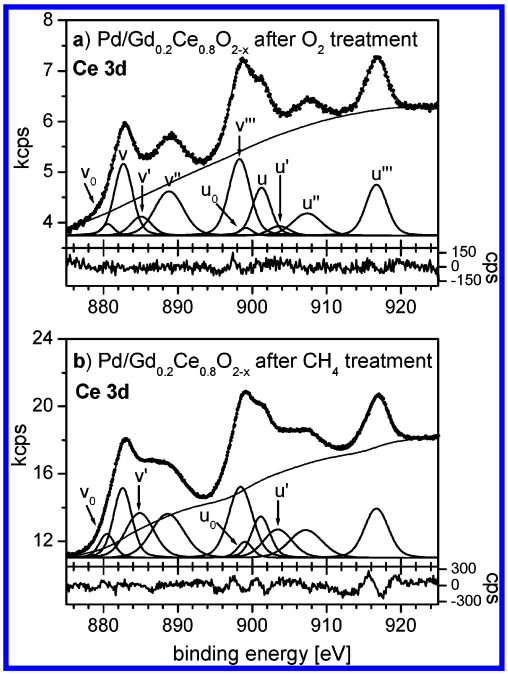

Figure 5. XPS Ce 3d spectra of the $Pd/Gd_{0.2}Ce_{0.8}O_{2-x}$ sample after oxygen (a) and methane (b) treatment. The increase in intensity of the doublet v′/u′ and the appearance of the doublet v_0/u_0 clearly indicate reduction of cerium ions upon treatment with methane.

a spin−orbit splitting of 32.0 eV. Two less intense doublets are present at higher binding energies. The satellite features a′ and a″ were observed at 1196.8 and 1199.5 eV, respectively, and the spin−orbit splitting was found to be 30.4 eV for the doublet a′/b′ and 32.9 eV for the doublet a″/b″. The peaks a_S and b_S are satellite lines, which are due to the use of a nonmonochromatic X-ray source.

Figure 4b shows an XPS O 1s spectrum for the gadolinium oxide sample. The spectrum is comprised of two components, where the main peak can be assigned to O^{2-} ions. The second peak is shifted by 2.6 eV to higher binding energy, and its relative intensity is ∼20%. In analogy to cerium and praseodymium oxides, this peak can be assigned to $O^{\delta-}$ species or OH groups.[21] The relatively high intensity indicates a considerable degree of disorder. This is also supported by the XRD data, which provided evidence for the coexistence of an amorphous phase (see section 3.1).

Gd 4d spectra were also recorded; the spectrum obtained for the pure gadolinium oxide sample is given as Supporting Information (Figure S1). While high-resolution studies of various Gd compounds revealed a well-resolved multiplet structure for the Gd 4d level,[29] our spectra were rather broad. The multiplet structure could not be resolved due to the limited experimental resolution and inhomogeneous broadening effects related to enhanced disorder in the nanostructured materials. Further analysis of the Gd 4d spectra was not reasonable here.

3.3.2. Gd-Doped Cerium Oxide. Several Gd-doped ceria samples were studied by XPS: a sample with 40% Gd content (without surface modification), two Pt-promoted samples with 20% and 40% Gd content, and two Pd-promoted samples with 20% and 40% Gd content. The samples were investigated after in situ treatments with oxygen and with methane. Ce 3d spectra were deconvolved into 10 peaks as described in our earlier study of Pr-doped ceria.[21] Values for the fitting parameters (see Supporting Information) were almost identical to those in the former study.

Figure 5 shows Ce 3d spectra of the Pd-promoted ceria sample doped with 20% Gd after oxygen (a) and methane (b) treatment. The spectra were deconvolved into five spin−orbit split doublets of Voigt functions labeled v_0/u_0, ..., v‴/u‴ in accordance with common use in the literature. While the peaks v, v″, v‴, u, u″, and u‴ are due to cerium ions in the +4 oxidation state, v_0, v′, u_0, and u′ reflect Ce^{3+} ions.[30,31] The observable increase in intensity of the doublet v′/u′ upon treatment with methane clearly shows the reduction of cerium ions for the sample presented in Figure 5. The relative amount of Ce^{3+} ions as calculated from the relative peak areas increases from ∼11% to ∼27% (see Table 2).

For the Pd-promoted sample with 40% Gd content, very similar results were found. Pt-promoted samples showed only a slight reduction of Ce cations upon the in situ methane treatment; for the Pt-promoted sample with 40% Gd content, the fraction of Ce cations in the +3 oxidation state increased from ∼2% to ∼13% (see Table 2). At first sight, this seems not much when compared to values reported for Pt-promoted ceria doped with Pr, but one has to note the different experimental conditions: while the Pr-doped samples had to be reduced ex situ in a flow reactor at ∼750 °C,[21] reduction of the Gd-doped ceria promoted by Pt could be observed even after in situ reduction at lower temperature (∼500 °C).

Comparing Gd-doped ceria promoted by Pt and Pd, one can notice stronger reduction of Ce cations in the case of surface modification with Pd. This is in agreement with the CH_4 TPR experiments, where the total amount of oxygen removed from the sample was also higher for the Pd-promoted samples (see section 3.2 and Table 3).

For the Gd-doped ceria sample without surface modification, no significant reduction was observed upon the in situ treatment with methane (see Table 2). The analysis revealed, however, that the amount of Ce^{3+} cations is extremely low in this sample after the oxygen treatment. The comparison with the pure CeO_2 sample provides experimental evidence for the assumption that doping with Gd reduces the number of Ce^{3+} cations, because oxygen vacancies move to the vicinity of the three-valent guest cations. To the best of our knowledge, this has not been

demonstrated by XPS before. Interestingly, the concentration of Ce^{3+} cations remains rather low after surface modification with Pt, but slightly exceeds the level found for undoped ceria when the surface is modified with Pd. This indicates that Pt and Pd interact in a different way with the surface and therefore differently affect the defect structure of the support.

As indicated in section 3.1, there is a clear correlation between the reducibility of the samples and the variation of the atomic Gd-to-Ce ratio in the oxidized and reduced samples as measured by quantitative XPS. Reduction of Ce cations is accompanied by a decrease in the Gd-to-Ce ratios (see Table 2). This provides evidence that Ce cations tend to segregate to the surface when they are reduced from the +4 to the +3 oxidation state.

The above analysis of Ce 3d spectra requires a remark related to the depth distribution of Ce^{3+} and Ce^{4+} ions in the samples. The intensity of photoemission peaks depends on the thickness of the layer through which the photoelectrons have to travel in the sample before detection. Therefore, the calculation of the relative amount of Ce^{3+} ions yields the accurate result only if the attenuation of the peaks associated with Ce^{3+} and Ce^{4+} ions is the same. Since there are indications that Ce^{3+} ions tend to segregate to the surface, the peaks corresponding to the +3 oxidation state may be less attenuated. As a consequence, the amount of Ce^{3+} ions may be systematically overestimated. Similar considerations were recently reported by Zhang et al. in a comparative XPS and XANES study of ceria nanoparticles.[32] Although it is in principle possible to perform calculations for a nonhomogeneous depth distribution of two species in spherical nanoparticles,[33] this is unfortunately not reasonable in the present case, because there is no concrete model that would predict to what extent Ce^{3+} ions really segregate to the surface. Therefore, the percentages calculated in the present work refer to the simple model, in which the Ce^{3+}-to-Ce^{4+} ratio is spatially constant. As a consequence, the Ce^{3+} amounts may be systematically overestimated, but the comparison of the results obtained for different samples and after different pretreatments remains of course meaningful.

Gd 3d spectra of the doped samples were basically similar to the spectrum shown in Figure 4a for pure gadolinium oxide. The binding energy of the main peak labeled "a" and the spin−orbit splitting for the doublet a/b were 1186.75 ± 0.3 eV and 32.05 ± 0.1 eV, respectively. The peaks a′ and a″ were observed at binding energies of 1197.0 ± 0.7 and 1199.4 ± 0.7 eV, respectively, and the spin−orbit splitting was found to be 30.1 ± 0.4 eV for the doublet a′/b′ and 33.1 ± 0.7 eV for the doublet a″/b″.

When comparing pure and doped samples, a slight difference can be observed in the relative intensity of the doublets a′/b′ and a″/b″ with respect to the main doublet a/b. Figure 6a shows a Gd 3d spectrum for the Pt-promoted ceria sample doped with 20% Gd. One can notice that the feature at ∼1198 eV is slightly more pronounced as compared to the pure gadolinium oxide sample. (The intensity ratio of the doublets a′/b′ and a″/b″ with respect to a/b was ∼0.2 for all Gd-doped ceria samples and ∼0.15 for the pure gadolinium oxide sample.) Variations of the relative intensity of the satellite feature at ∼1198 eV were also observed by Szade and Neumann in a comparison of metallic gadolinium and GdF_3.[34] While the feature was well pronounced for metallic Gd, it was nearly absent in the case of GdF_3. The lack of conduction electrons in GdF_3 was supposed to influence the excitations responsible for the satellite feature.[34] The observation that the satellite feature is slightly more pronounced in the case of Gd-doped ceria than in gadolinium oxide therefore suggests that Gd has a partly metallic character in the doped

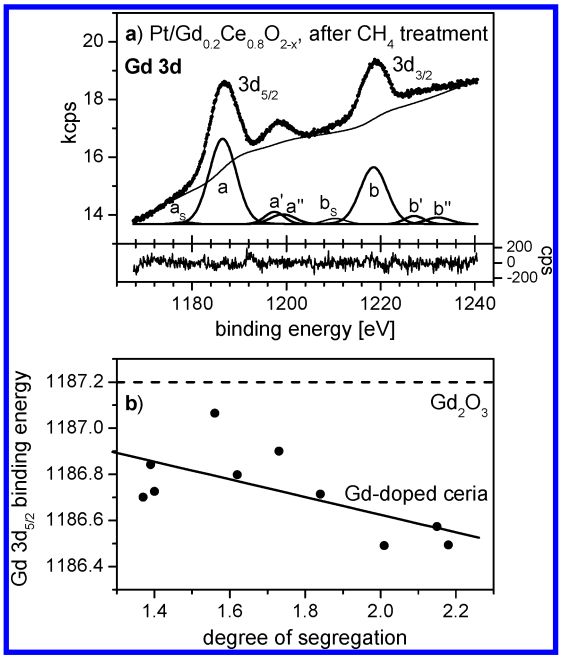

Figure 6. (a) XPS Gd 3d spectrum of the $Pt/Gd_{0.2}Ce_{0.8}O_{2-x}$ sample after treatment with methane. (b) Dependence of the binding energy of the main Gd $3d_{5/2}$ peak "a" on the degree of segregation, which has been defined as the ratio of the atomic Gd-to-Ce ratio as measured by XPS (see Table 2) to the overall stoichiometric Gd-to-Ce ratio (0.25 for samples with 20% Gd content and 0.67 for samples containing 40% Gd). A trend line has been added for the doped samples (solid line), and the binding energy observed for pure gadolinium oxide is included for comparison (dashed line).

samples, possibly because of the formation of Gd clusters at the surface due to the pronounced segregation effect. Conduction electrons of the doped ceria lattice might also favor the excitation of the satellite feature.

Indications for the formation of Gd clusters at the surface due to segregation are also provided by the observation of slight variations in the binding energy of the main peak "a". According to the *Handbook of X-ray Photoelectron Spectroscopy* edited by Wagner et al.,[23] the binding energy of the main peak should be ∼1187 eV for elemental Gd and ∼1189 eV for the oxide. Figure 6b shows the observed binding energy position as a function of the degree of segregation, which has been defined as the ratio between the experimental Gd-to-Ce ratio and the theoretical ratio for the case of homogeneous spatial distribution of the guest cations in the host lattice (see Table 2). The binding energy found for pure gadolinium oxide is included in the figure for comparison (dashed line). Binding energies were found to be lower for the doped samples than for the pure gadolinium oxide sample, and there is a trend for the binding energy of the main peak to decrease slightly when the segregation effect is more strongly pronounced (solid trend line). This suggests a more metallic character at high degrees of segregation.

One has to mention that the above considerations are complicated by the fact that values reported for the binding energy of the main $3d_{5/2}$ peak of Gd_2O_3 can significantly differ. While the *Handbook of X-ray Photoelectron Spectroscopy* gives a value of ∼1189 eV,[23] other literature sources report lower values down to 1186.8 eV.[28,35] Comparison with the Gd_2O_3 sample studied in this work is also difficult, because the different charge references for pure and doped samples introduce uncertainties. Therefore, the above considerations can be understood only as a possible interpretation.

The trend observed for the binding energy can also be analyzed, taking into account the specificity of the local

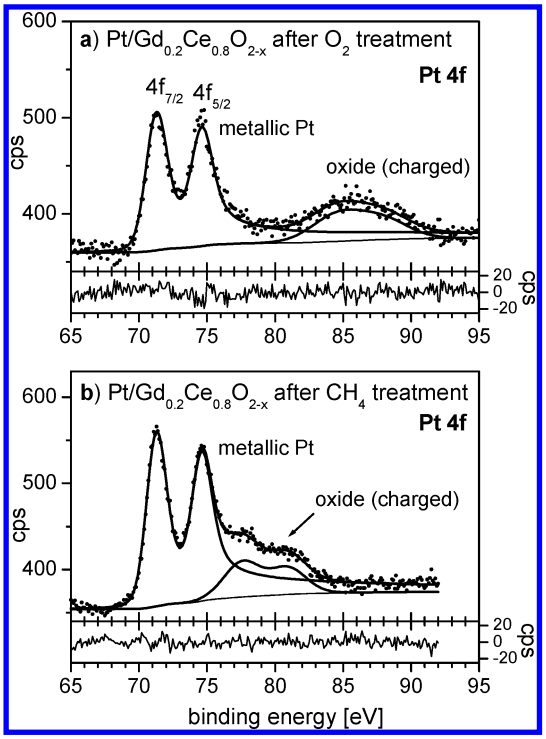

Figure 7. XPS Pt 4f spectra of the $Pt/Gd_{0.2}Ce_{0.8}O_{2-x}$ sample after oxygen (a) and methane (b) treatment. The binding energy scale has *not* been corrected for charging. While the peaks corresponding to oxidized platinum are shifted like the corresponding Ce 3d spectra, a metallic phase is observed without charging.

environment (coordination) of Gd cations in pure gadolinia (distorted 6-fold coordination) and in ceria as substituting cations (8-fold coordination). The effective charge of cations with the same oxidation number is well-known to depend on the type of the oxygen polyhedra: the higher the Me−O coordination number is, the lower the positive charge of the central cation is. When the effective charge is lower, the electrons are less strongly bound in the central cation. Thus, a lower binding energy for photoelectrons emitted from Gd cations as a dopant in the ceria lattice seems reasonable. The trend for the further decrease in the binding energy with increasing degree of segregation can tentatively be explained by electrostatic effects due to the increase in the average number of Me^{3+} cations as next-nearest neighbors, which should lead to an increase in the electron density on Gd cations. Moreover, segregation is expected to cause the appearance of some anion vacancies in the coordination sphere of Gd cations,[26] which also could further decrease the effective charge on Gd cations.

Apart from the analysis of cerium and gadolinium states, the study of Pt and Pd is of special interest. XPS Pt 4f spectra of the sample with 20% Gd content after oxidation and after treatment with methane are presented in Figure 7, where the energy scale has *not* been corrected for charging. A rather unusual situation is observed here: Two spin−orbit split doublets of Pt peaks are present, with one doublet being shifted due to charging and the other doublet not. The species with the $4f_{7/2}$ peak centered at 71.2 eV can clearly be identified as metallic platinum.[36] The asymmetry parameter is 0.15 for that component in the presented fits. A second species is observed at higher binding energy. This component is shifted like the corresponding Ce 3d spectra due to the charging effect. When subtracting the corresponding energy shifts (11.4 and 5.5 eV), binding energies of 73.2 and 72.1 eV are obtained for the Pt $4f_{7/2}$ peaks after the oxidation and the methane treatment, respectively. Thus, the second peak corresponds to oxidized Pt. The shift of the corrected binding energies indicates a transition from Pt^{2+} to Pt^{+} upon reduction with methane.[21] Distinct peaks corresponding to the different oxidation states cannot be resolved, however, due the high noise level. The unusual observation that one Pt species (ionic Pt) is subjected to the overall charging effect, while the other one (metallic Pt) is found at the usual binding energy for bulk platinum suggests the formation of two phases: oxidized Pt ions strongly bound to the doped ceria grains and small metallic Pt clusters. To verify the existence of two phases, we investigated the sample also by XRD. A distinct metallic platinum phase could not be detected, however, which means that eventually present Pt clusters must be very small.

The oxidation states of Pt were also studied by FTIR spectroscopy of adsorbed CO (see Figure 8). For Gd-doped ceria samples without Pt or Pd, two bands are observed in the carbonyl stretching range at ∼2169 and ∼2120 cm^{-1} (Figure 8a,d). These bands can be assigned to linear adsorption of CO to Ce^{4+} and Me^{3+} (Me = Ce, Gd) cations, respectively.[18,37−39] Surface modification with Pt leads to a strong additional band at ∼2178 cm^{-1} corresponding to CO linearly adsorbed on Pt^{2+} ions (Figure 8b,e).[18,37] Furthermore, a less intense, broad band is observed at ∼2050 cm^{-1}, which indicates the presence of metallic platinum.[18,37,40,41] As shown by Bourane and Bianchi in a study of Pt/Al_2O_3 catalysts, the position of this band depends on the dispersion of Pt.[42] With increasing dispersion, the IR band corresponding to Pt^0 shifts to lower wavenumbers. At 300 K, a band position of 2054 cm^{-1} was reported for a dispersion of 0.75.[42] Since the band shifts also to lower wavenumbers with increasing temperature, the position of the Pt^0 band observed at ∼2050 cm^{-1} in our case at 77 K indicates a dispersion definitely higher than 0.75 and thus confirms that the metallic Pt clusters are indeed very small.

When comparing the FTIR spectra of the samples with 20% and 40% Gd content, one can note that the band corresponding to Pt^0 is less pronounced for the sample with the higher dopant content. In agreement with this observation, no metallic Pt could be detected by XPS for the sample with 40% Gd content (see Figure 9). Only one doublet of peaks corresponding to oxidized Pt ions was observed with the Pt $4f_{7/2}$ peak centered at about 72 eV (corrected for charging). Deconvolution of the spectra into contributions from Pt^{2+} and Pt^{+} was not possible due to the low Pt content of only 1.4 wt %, which implies a high noise level.

Comparing the two Pt-promoted samples with 20% and 40% Gd content, quantitative analysis reveals one more difference: calculation of the atomic ratio of platinum to cerium and gadolinium from the XPS peak areas yielded ∼1.5% for the sample containing 40% Gd, but ∼6% for the sample with 20% Gd content. Since the amount of Pt used in the synthesis was 1.4 wt % in both cases, this indicates for the $Pt/Gd_{0.2}Ce_{0.8}O_{2-x}$ sample that Pt has segregated to the surface. This is consistent with the observation that small metallic Pt clusters were formed in this case. In contrast, for the sample with the higher content of Gd, incorporation of Pt cations into the surface layer of the Gd-doped ceria support can be suggested. This agrees with the decline of the intensity of the Pt^{2+}−CO band in this case (compare Figure 8b,e). At 40% dopant content the surface is strongly enriched with gadolinium cations due to the segregation effect. Therefore, the observed indications for penetration of Pt^{2+} into the surface layer suggest that the Pt^{2+} cations prefer the vicinity of cerium cations.

XPS Pd 3d spectra are shown for the $Pd/Gd_{0.2}Ce_{0.8}O_{2-x}$ sample in Figure 10. After the oxidative pretreatment two

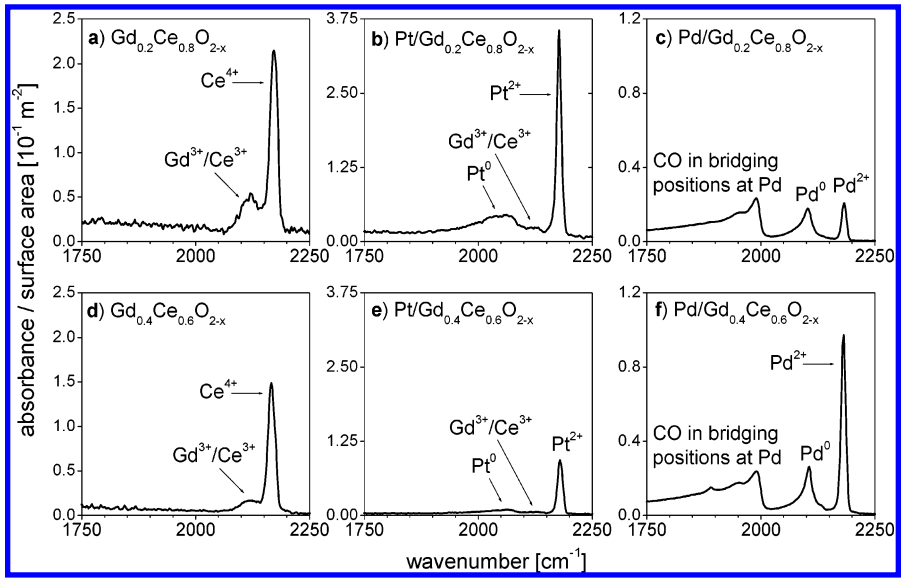

Figure 8. FTIR spectra of fresh Gd-doped ceria samples after exposure to 16 μmol (per pellet) of carbon monoxide. (a, d) Gd-doped ceria samples with 20% and 40% Gd content; (b, e) Gd-doped ceria samples modified with Pt; (c, f) Gd-doped ceria samples modified with Pd.

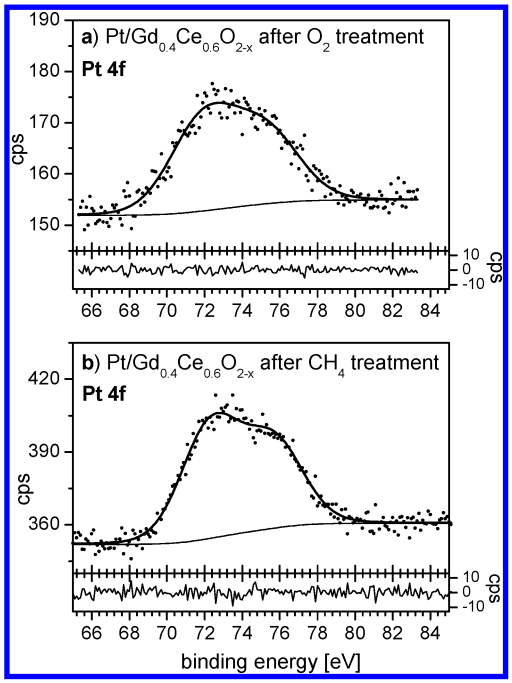

Figure 9. XPS Pt 4f spectra of the $Pt/Gd_{0.4}Ce_{0.6}O_{2-x}$ sample after oxygen (a) and methane (b) treatment. For this sample, no metallic Pt is observed.

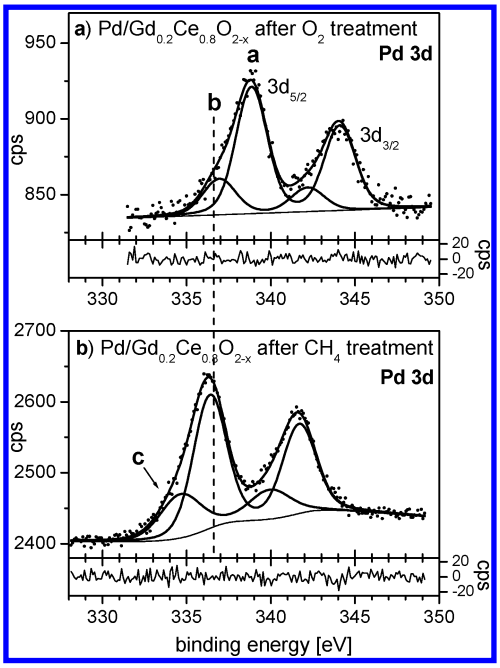

Figure 10. XPS Pd 3d spectra of the $Pd/Gd_{0.2}Ce_{0.8}O_{2-x}$ sample after oxygen (a) and methane (b) treatment.

doublets of Voigt functions were required to obtain a good fit. The $3d_{5/2}$ peaks of the two components "a" and "b" are centered at 338.9 and 336.9 eV, respectively. Upon reduction with methane, peak a disappears while peak b rises in intensity and shifts to slightly lower binding energy (336.4 eV). Additionally, a new peak "c" at 334.6 eV appears. Peaks b and c can be assigned to PdO and metallic Pd, respectively.[43,44] The origin of the component "a" with the highest binding energy is not as clear. Recently, a similar Pd $3d_{5/2}$ feature was observed at 337.7 eV for La-doped Pd/CeO_2 catalysts.[45] This binding energy value is significantly higher than that usually reported for PdO and implies the presence of Pd^{2+} ions that are much more cationic than in PdO. Pd^{2+} species with highly cationic character could be formed by strong metal−support interaction (SMSI) effects,[45] where the Pd−O bonding belongs not to Pd−O−Pd but rather to Pd−O−Ce or Pd−O−Gd configurations at the $Pd/Ce_{1-x}Gd_xO_{2-y}$ interface. Unusually high Pd $3d_{5/2}$ binding energies were also observed in a recent study of $Pd/\gamma\text{-}Al_2O_3$ catalysts and attributed to deficiently coordinated PdO, which is highly dispersed Pd in intimate contact with the support.[46] The drastic changes in the spectra upon the treatment with methane indicate that palladium is easily oxidized and reduced in the presence of Gd-doped ceria.

The Pd-promoted catalysts were also studied by FTIR spectroscopy of adsorbed CO molecules. The spectra revealed three pronounced bands at ∼2182, ∼2105, and ∼1990 cm^{-1} for the samples modified with Pd (see Figure 8c,f). According to FTIR studies of Pd-based catalysts, bands at 2145, 2107, and 2060 cm^{-1} can be assigned to carbonyl species linearly adsorbed on Pd surface sites with palladium present as Pd^{2+}, Pd^{+}, and Pd^{0}, respectively.[39,47] Other interpretations of these bands can be made on the basis of previous surface science studies of the CO/Pd(111) system which have shown that bands near 1850, 1950, and 2100 cm^{-1} correspond to CO adsorbed on 3-fold

hollow sites, CO in bridging positions, and linearly (on-top) adsorbed CO, respectively.[48−50] CO adsorbed on the surface of palladium particles grown on a thin film of alumina (Pd/Al_2O_3/NiAl(110)) has been characterized by C−O stretching frequencies of 1970 and 2110 cm^{-1}, which correspond to CO in bridging positions and linearly adsorbed CO, respectively.[48] According to these literature data[37,48−51] and taking into account also our XPS data, we assign the bands around ∼1990 and ∼2105 cm^{-1} to bridge-bonded and on-top CO species over metallic palladium particles, respectively. The high-frequency band at ∼2182 cm^{-1}, which is observed for the Pd-modified samples in this work, can be assigned to CO linearly adsorbed on Pd^{2+} ions.[37,39,47]

The intensity of the Pd^{2+}−CO band is considerably higher for the sample with the higher Gd content (compare Figure 8c,f). This result is at least qualitatively supported by quantitative analysis of the XPS data. The atomic ratio of palladium to cerium and gadolinium, as calculated from the total peak areas of spectra recorded after the oxidation treatment, turned out to be ∼4.0% for the sample with 20% Gd content and ∼4.6% for the sample with 40% Gd content. Thus, in contrast to Pt^{2+} cations which exposed a tendency for incorporation into the surface layer of the support, Pd^{2+} cations seem to be *enriched* on the surface at high Gd content.

Finally, on the basis of our results obtained for the Pt and Pd states, we can briefly comment on the question of why surface modification with Pd has a stronger effect on the reducibility of the doped ceria support by methane. The XPS study revealed that Pd occurs in a highly cationic state which is presumably due to strong metal−support interactions. Since no analogue was observed for the Pt-promoted system, this highly cationic Pd species might be responsible for the higher reducibility. Furthermore, the amount of metal *cations* accessible for the methane molecules seems to be higher in the Pd-promoted system, because Pt^{2+} cations tend to be partly incorporated into the surface layer of the support. As shown by the comparison of the two Pt-promoted samples, the oxidation states of the noble metals can also be strongly influenced by the Gd content of the support. Influencing the metal−support interactions by choosing the kind and amount of dopant ions seems to be a promising prospect for controlling the catalytic properties of the nanostructured, doped ceria system prepared by the Pechini method.

4. Summary

Various nanostructured cerium dioxide samples doped with gadolinium were prepared by the Pechini method, optionally modified with Pt or Pd, and investigated by a combination of techniques to study correlations between the structural, electronic, and chemical properties. Studies of the chemical behavior focused on the interaction with methane, which is relevant for applications such as syngas production by partial oxidation of methane.

CH_4 TPR experiments showed that surface modification with noble metals strongly favors the generation of synthesis gas at moderate temperatures. While for samples without surface modification up to ∼750 °C mainly deep oxidation of methane to carbon dioxide occurs, for samples modified with Pt or Pd already at temperatures around ∼500 °C the desired reaction of partial oxidation of methane dominates. Comparing Pt- and Pd-promoted samples, the experiments revealed a higher total conversion rate during the TPR run for the Pd-promoted samples.

XPS investigations after in situ treatments of the samples with oxygen and methane in the preparation chamber of the spectrometer are in good agreement with the TPR results. Methane treatments carried out at ∼500 °C resulted in a significant reduction of Ce cations only for samples modified with noble metals, with the effect being more pronounced for Pd-promoted samples than for Pt-promoted samples.

Quantitative XPS and SIMS revealed a certain degree of segregation of Gd cations at the surface of all samples. The degree of segregation was found to decrease slightly upon reduction of the samples with methane; the effect was more pronounced for samples that were more strongly reduced. This behavior can be explained by the segregation of Ce cations to the surface when they are reduced from the +4 to the +3 oxidation state. This result is in contrast to Pr-doped ceria, where enhanced segregation of *guest* cations was observed after reduction with methane, because Pr tends to segregate to the surface when reduced from Pr^{4+} to Pr^{3+}.[21]

Photoemission spectra of Pt and Pd core levels indicated that Pd interacts more strongly with the doped ceria support. The presence of highly cationic Pd species might be responsible for the higher reducibility of the doped ceria when compared to the Pt-promoted system. A specificity was observed for the Pt-promoted sample with 20% Gd content for which a second phase of very small Pt clusters was revealed by XPS. It is a promising approach to controlling the catalytic properties of the nanostructured doped ceria system prepared by the Pechini method by tuning the degree of the metal−support interaction.

Acknowledgment. This work was partially supported by the INTAS 01-2162 and ISTC 2529 Projects, the Integration Project 39 of SB RAS, and the NATO SFP Project 980878. H.B. is grateful for support by a fellowship within the Postdoc program of the German Academic Exchange Service (DAAD). Furthermore, the authors would like to thank S. N. Trukhan and V. P. Ivanov for SIMS measurements.

Supporting Information Available: Fitting details for the analysis of XPS Ce 3d spectra; XPS Gd 4d spectrum for the pure gadolinium oxide sample. This material is available free of charge via the Internet at http://pubs.acs.org.

References and Notes

(1) He, H.; Dai, H. X.; Ng, L. H.; Wong, K. W.; Au, C. T. *J. Catal.* **2002**, *206*, 1.
(2) Yao, C.-S.; Weng, H.-S. *Ind. Eng. Chem. Res.* **1998**, *37*, 2647.
(3) Concepcion, P.; Corma, A.; Silvestre-Albero, J.; Franco, V.; Chane-Ching, J. *J. Am. Chem. Soc.* **2004**, *126*, 5523.
(4) Haile, S. M. *Mater. Today* **2003**, *6*, 24.
(5) Sammells, A. F.; Schwartz, M.; Mackay, R. A.; Barton, T. F.; Peterson, D. R. *Catal. Today* **2000**, *56*, 325.
(6) Ishihara, T.; Takita, Y. *Catal. Surv. Jpn.* **2000**, *4*, 125.
(7) Kharton, V. V.; Yaremchenko, A. A.; Naumovich, E. N.; Marques, F. M. B. *J. Solid State Electrochem.* **2000**, *4*, 243.
(8) Kilner, J. A. *Solid State Ionics* **2000**, *123*, 13.
(9) Skinner, S.; Kilner, J. A. *Mater. Today* **2003**, *6*, 30.
(10) Tschöpe, A.; Ying, J. Y.; Tuller, H. L. *Sens. Actuators, B* **1996**, *31*, 111.
(11) Chiang, Y.-M.; Lavik, E. B.; Kosacki, I.; Tuller, H. L.; Ying, J. Y. *J. Electroceram.* **1997**, *1*, 7.
(12) Valenzuela, R. X.; Bueno, G.; Solbes, A.; Martinez, E.; Cortez Corberan, V. *Top. Catal.* **2001**, *15*, 181.
(13) Wang, Z. L.; Feng, X. *J. Phys. Chem. B* **2003**, *107*, 13563.
(14) Deshande, A. S.; Pinna, N.; Beato, P.; Antonietti, M.; Niederberger, M. *Chem. Mater.* **2004**, *16*, 2599.
(15) Sadykov, V. A.; Kuznetsova, T. G.; Alikina, G. M.; Frolova, Y. V.; Lukashevich, A. I.; Potapova, Y. V.; Muzykantov, V. S.; Rogov, V. A.; Kriventsov, V. V.; Kochubei, D. I.; Moroz, E. M., Zyuzin, D. I.; Zaikovskii, V. I.; Kolomiichuk, V. N.; Paukshtis, E. A.; Burgina, E. B.; Zyryanov, V. V.; Uvarov, N. F.; Neophytides, S.; Kemnitz, E. *Catal. Today* **2004**, *93*−*95*, 45.
(16) Sadykov, V. A.; Frolova, Yu. V.; Alikina, G. M.; Lukashevich, A. I.; Muzykantov, V. S.; Rogov, V. A.; Moroz, E. M.; Zyuzin, D. A.; Ivanov,

V. P.; Borchert, H.; Paukshtis, E. A.; Bukhtiyarov, V. I.; Kaichev, V. V.; Neophytides, S.; Kemnitz, E.; Scheurell, K. *React. Kinet. Catal. Lett.* **2005**, *86*, 21.

(17) Sadykov, V. A.; Frolova, Yu. V.; Alikina, G. M.; Lukashevich, A. I.; Neophytides, S. *React. Kinet. Catal. Lett.* **2005**, *86*, 29.

(18) Sadykov, V. A.; Frolova, Yu. V.; Alikina, G. M.; Lukashevich, A. I.; Muzykantov, V. S.; Rogov, V. A.; Moroz, E. M.; Zyuzin, D. A.; Ivanov, V. P.; Borchert, H.; Paukshtis, E. A.; Bukhtiyarov, V. I.; Kaichev, V. V.; Neophytides, S.; Kemnitz, E.; Scheurell, K. *React. Kinet. Catal. Lett.* **2005**, *85*, 367.

(19) Sadykov, V. A.; Frolova, Yu. V.; Alikina, G. M.; Lukashevich, A. I.; Neophytides, S. *React. Kinet. Catal. Lett.* **2005**, *85*, 375.

(20) Pechini, M. P. Method of preparing lead and alkaline earth titanates and niobates and coating method using the same to form a capacitor. U.S. Patent 3,330,697, July 11, 1967.

(21) Borchert, H.; Frolova, Yu. V.; Kaichev, V. V.; Prosvirin, I. P.; Alikina, G. M.; Lukashevich, A. I.; Zaikovskii, V. I.; Moroz, E. M.; Trukhan, S. N.; Ivanov, V. P.; Paukshtis, E. A.; Bukhtiyarov, V. I.; Sadykov, V. A. *J. Phys. Chem. B* **2005**, *109*, 5728.

(22) Frolova, Yu. V. Synthesis and investigation of the physicochemical properties of catalysts based on complex oxides and zirconium phosphates for oxidation of hydrocarbons. Ph.D. Thesis, Novosibirsk State University, 2004 (in Russian).

(23) *Handbook of X-ray Photoelectron Spectroscopy*; Wagner, C. D., Riggs, W. M., Davis, L. E., Moulder, J. F., Muilenberg, G. E., Eds.; Perkin-Elmer Corporation: Eden Prairie, MN, 1979.

(24) Ilinitsch, O. M.; Nosova, L. V.; Gorodetskii, V. V.; Ivanov, V. P.; Trukhan, S. N.; Gribov, E. N.; Bogdanov, S. V.; Cuperus, F. P. *J. Mol. Catal., A* **2000**, *158*, 237.

(25) McBride, J. R.; Hass, K. C.; Poindexter, B. D.; Weber, W. H. *J. Appl. Phys.* **1994**, *76*, 2435.

(26) Sadykov, V. A.; Frolova, Yu. V.; Kriventsov, V. V.; Kochubei, D. I.; Moroz, E. M.; Zyuzin, D. A.; Potapova, Yu. V.; Muzykantov, V. S.; Zaikovskii, V. I.; Burgina, E. B.; Borchert, H.; Trukhan, S. N.; Ivanov, V. P.; Neophytides, S.; Kemnitz, E.; Scheurell, K. *Mater. Res. Soc. Symp. Proc.* **2005**, *835*, K3.6.

(27) Sarma, D. D.; Rao, C. N. R. *J. Electron Spectrosc. Relat. Phenom.* **1980**, *20*, 25.

(28) Uwamino, Y.; Ishizuka, T.; Yamatera, H. *J. Electron Spectrosc. Relat. Phenom.* **1984**, *34*, 67.

(29) Szade, J.; Lachnitt, J.; Neumann, M. *Phys. Rev. B* **1997**, *55*, 1430.

(30) Romeo, M.; Bak, K.; El Fallah, J.; Le Normand, F.; Hilaire, L. *Surf. Interface Anal.* **1993**, *20*, 508.

(31) Hardacre, C.; Roe, G. M.; Lambert, R. M. *Surf. Sci.* **1995**, *326*, 1.

(32) Zhang, F.; Wang, P.; Koberstein, J.; Khalid, S.; Chan, S.-W. *Surf. Sci.* **2004**, *563*, 74.

(33) McGinley, C.; Borchert, H.; Pflughoefft, M.; Al Moussalami, S.; de Castro, A. R. B.; Haase, M.; Weller, H.; Möller, T. *Phys. Rev. B* **2001**, *64*, 245312.

(34) Szade, J.; Neumann, M. *J. Phys.: Condens. Matter* **2001**, *13*, 2717.

(35) Flückiger, T.; Erbudak, M.; Hensch, A.; Weisskopf, Y.; Hong, M.; Kortan, A. R. *Surf. Interface Anal.* **2002**, *34*, 441.

(36) Powell, C. J. *Appl. Surf. Sci.* **1995**, *89*, 141.

(37) Hadjiivanov, K. I.; Vayssilov, G. N. *Adv. Catal.* **2002**, *47*, 307.

(38) Binet, C.; Daturi, M.; Lavalley, J.-C. *Catal. Today* **1999**, *50*, 207.

(39) Craciun, R.; Daniell, W.; Knözinger, H. *Appl. Catal. A* **2002**, *230*, 153.

(40) Rupprechter, G.; Dellwing, T.; Unterhalt, H.; Freund, H.-J. *J. Phys. Chem. B* **2001**, *105*, 3797.

(41) Perrichon, V.; Retailleau, L.; Bazin, P.; Daturi, M.; Lavelley, J. C. *Appl. Catal., A* **2004**, *260*, 1.

(42) Bourane, A.; Bianchi, D. *J. Catal.* **2003**, *218*, 447.

(43) Brun, M.; Berthet, A.; Bertolini, J. C. *J. Electron Spectrosc. Relat. Phenom.* **1999**, *104*, 55.

(44) Monteiro, R. S.; Zemlyanov, D.; Storey, J. M.; Ribeiro, F. H. *J. Catal.* **2001**, *201*, 37.

(45) Sun, K.; Lu, W.; Wang, M.; Xu, X. *Appl. Catal., A* **2004**, *268*, 107.

(46) Ihm, S.-K.; Jun, Y.-D.; Kim, D.-C.; Jeong, K.-E. *Catal. Today* **2004**, *93*−*95*, 149.

(47) Tessier, D.; Rakai, A.; Bozon-Verduras, F. *J. Chem. Soc., Faraday Trans.* **1992**, *88*, 741.

(48) Dellwing, T.; Rupprechter, G.; Unterhalt, H.; Freund, H.-J. *Phys. Rev. Lett.* **2000**, *85*, 776.

(49) Kaichev, V. V.; Prosvirin, I. P.; Bukhtiyarov, V. I.; Unterhalt, H.; Rupprechter, G.; Freund, H.-J. *J. Phys. Chem. B* **2003**, *107*, 3522.

(50) Kaichev, V. V.; Morkel, M.; Unterhalt, H.; Prosvirin, I. P.; Bukhtiyarov, V. I.; Rupprechter, G.; Freund, H.-J. *Surf. Sci.* **2004**, *566*−*568*, 1024.

(51) Tarasov, A. L.; Shvez, V. A.; Kasanskij, V. B. *Kinet. Katal.* **1989**, *30*, 396 (in Russian).